ISSN 1063-7710, Acoustical Physics, 2010, Vol. 56, No. 6, pp. 1067–1079. © Pleiades Publishing, Ltd., 2010.
Original Russian Text © I.P. Smirnov, I.R. Smirnova, A.I. Khil'ko, 2010, published in Akusticheskiĭ Zhurnal, 2010, Vol. 56, No. 6, pp. 813–825.

OCEAN ACOUSTICS.
HYDROACOUSTICS

Optimization of Mode Composition of the Acoustic Field Excited by a Vertical Antenna Array in a Shallow Sea

I. P. Smirnov, I. R. Smirnova, and A. I. Khil'ko

Institute of Applied Physics, Russian Academy of Sciences, ul. Ulyanova 46, Nizhni Novgorod, 603950 Russia
e-mail: A.khil@hydro.appl.sci-nnov.ru

Received January 12, 2010

Abstract—The problem statement is described, and the solution to the problem of optical tuning of the radiating antenna array providing for the optimal mode composition of the field radiated to a waveguide is determined. Matlab software is developed based on the proposed algorithms, and the optimal fields for shallow sea waveguides are calculated.

DOI: 10.1134/S1063771010060333

1. INTRODUCTION

One of the promising methods of remote diagnostics of shallow water inhomogeneities is low-frequency small-mode acoustic tomography [1–3]. Its implementation is related to selective excitation and reception of small-mode acoustic signals. The sensitivity of the method is mainly determined by the quality of such selection. Radiator arrays where amplitude-phase distributions required for excitation of corresponding modes are created served as an effective instrument for generation of small-mode signals. The mode composition of the radiated fields at a specified position of the array in a waveguide depends on the method of excitation of individual radiators. When moving away from the antenna, the losses attributed to the interaction of individual modes with the bottom and their scattering at the wind-induced waves on the free surface start playing an important role in the mode spectrum formation. The limitation of the antenna aperture, as well as oscillations of the radiators in horizontal planes owing to underwater flows, yields an undesirable broadening of the mode spectrum when unnecessary (parasitic) modes are actively excited along with the necessary modes.

A numerical analysis of peculiarities of small-mode field generation in a shallow sea for the array with deflecting radiators was done in [6–8]. It is shown that radiator oscillations yield anisotropy of the radiated mode composition in a horizontal plane and a dependence of the intensities of individual modes on the direction of their propagation. The present work, which is a continuation of these investigations, studies potential possibilities of forming an assigned mode composition of the field in a shallow sea related to an appropriate selection of an acceptable way of sound source excitation. In particular, it has solved the problems of determining excitation coefficients providing for the maximal total intensity of a specified group of modes at a given point of a waveguide, the minimal intensity of parasitic modes, the maximal ratio of intensities of the given groups of modes, etc. This work can be also considered as a development of [9], where some problems of optimization of the waveguide field mode composition were solved.

2. MODE REPRESENTATION OF THE FIELD OF A GROUP OF INDEPENDENT RADIATORS

Consider an antenna array consisting of K independent point monochromatic radiators of the sound with the frequency ω positioned at the points $\vec{R}_k = (x_k, y_k, z_k)$, $k = 1 \ldots K$. Such a collective source can be written as

$$u(\vec{r}) = \sum_{k=1}^{K} C_k \delta(\vec{r} - \vec{R}_k),$$

where $\delta(\vec{r})$ is the delta function and C_k is the complex excitation coefficient of the kth radiator. For the spectral amplitude of the total field generated by the antenna array at the observation point $\vec{r}_0 = (\vec{e}_0, r_0, z_0)$ positioned at the distance r_0 in the direction of the unit vector $\vec{e}_0$ in a horizontal plane, we have an approximate representation in the form of the sum of $N_{\max}$ weakly attenuating modes,

$$\Phi_0(\vec{r}_0, \omega) = \sum_{j \le N_{\max}} A_j(\vec{e}_0)\psi_j(z_0)\frac{\exp(ik_j - \varsigma_j)r_0}{\sqrt{k_j r_0}}. \quad (1)$$

Here $\psi_j = \psi_j(z, \omega)$ is the normalized profile of the jth mode, $k_j = k_j(\omega)$ is the spectral number, and $\varsigma_j = \varsigma_j(\omega)$ is the attenuation decrement of the jth mode [10]. When deriving Eq. (1) in [6], it was assumed that the deflection of sources in the horizon-

tal planes from the origin $\vec{\rho}_k = (x_k, y_k)$ are negligible, $k_j|\vec{\rho}_k|^2 \ll \pi r_0$ for all $j \le N_{\max}$ and $1 \le k \le K$. At that, the mode amplitudes

$$A_j(\vec{e}_0) = \sum_{k=1}^{K} C_k \phi^{(j)*}(\vec{R}_k, \vec{e}_0, \omega),$$
$$\varphi^{(j)}(\vec{R}_k, \vec{e}_0, \omega) \equiv \exp\{ik_j\langle\vec{\rho}_k, \vec{e}_0\rangle\}\psi_j(z_k, \omega)\sqrt{\pi(i+1)} \quad (2)$$

depend on the frequency ω, the excitation coefficients C_k, the coordinates of the sources $\vec{R}_k$, and the direction $\vec{e}_0$ to the observation point in a horizontal plane (the asterisk means complex conjugation). The intensity of the jth mode at the point $\vec{r}_0$ is determined by the equation

$$W_j(\vec{r}_0) = |A_j(\vec{e}_0)|^2 |\psi_j(z_0)|^2 \frac{\exp(-2\varsigma_j r_0)}{k_j r_0}. \quad (3)$$

Introducing into consideration the complex unitary space C^K (above the field of complex numbers) with the scalar product $\langle\vec{u}, \vec{v}\rangle = \sum_{k=1}^{K} u_k \nabla_k^*$ and the norm $|\vec{u}| = \sqrt{\langle\vec{u}, \vec{u}\rangle}$, we write amplitudes (2) in the form of scalar products $A_j(\vec{e}_0) = \langle\vec{C}, \vec{\phi}^{(j)}(\vec{e}_0)\rangle$ and mode intensity (3) at the points $\vec{r}_0$ as

$$W_j(\vec{r}_0) = \left|\langle\vec{C}, \vec{\zeta}^{(j)}(\vec{r}_0)\rangle\right|^2,$$
$$\vec{\zeta}^{(j)}(\vec{r}_0) \equiv \psi_j(z_0)\frac{\exp(-\varsigma_j r_0)}{\sqrt{k_j r_0}}\vec{\phi}^{(j)}(\vec{e}_0). \quad (4)$$

Here the vectors are $\vec{C} = \{C_1, \ldots, C_K\}$, $\vec{\phi}^{(j)}(\vec{e}_0) \equiv \left\{\phi^{(j)}(\vec{R}_1, \vec{e}_0), \ldots, \phi^{(j)}(\vec{R}_K, \vec{e}_0)\right\}$.

3. OPTIMIZATION OF THE MODE COMPOSITION OF THE FIELD

During all statements of the problems of optimal field generation, we will proceed from the fact that the total power of the sources feeding the radiators does not exceed the specified value. We will denote the set of all vectors of excitation coefficients $\vec{C} = \{C_1, \ldots, C_K\}$ at which this condition is fulfilled as $£ = \{\vec{C} : |\vec{C}| \le C_0\}$, where C_0 is the specified number.

Let us consider the direction $\vec{e}_0$ in a horizontal plane and the observation point $\vec{r}_0 = (\vec{e}_0, r_0, z_0)$ positioned in this direction from the source at the distance r_0 and the depth z_0. Assume that, according to the content of the problem to be solved, the set of all modes is divided at the given point into two classes. The modes of the first class are considered useful; those of the second class, useless (parasitic). Corresponding sets of mode indices will be denoted as M and L. Denote (total) intensities (4) of useful and parasitic modes at the observation point as

$$W_M = \sum_{m\in M} W_m(\vec{r}_0) = \sum_{m\in M} \left|\langle\vec{\zeta}^{(m)}(\vec{r}_0), \vec{C}\rangle\right|^2,$$
$$W_L = \sum_{l\in L} W_l(\vec{r}_0) = \sum_{l\in L} \left|\langle\vec{\zeta}^{(l)}(\vec{r}_0), \vec{C}\rangle\right|^2. \quad (5)$$

Let us consider the following three problems of optimization of the mode composition of the field related to the selection of excitation coefficients of radiators:

$$W_M(\vec{C}) \to \max_{\vec{C}\in£}, \quad (6)$$

$$W_L(\vec{C}) \to \min_{\vec{C}\in£}, \quad (7)$$

$$\begin{cases} W_M(\vec{C}) \to \max_{\vec{C}\in£}, \\ W_L(\vec{C}) \to \min_{\vec{C}\in£}. \end{cases} \quad (8)$$

The *M*-problem (6) of the generation of the field with the maximal intensity of useful modes at the point $\vec{r}_0$. If the set of useful modes M consists of a number of the only mode m_0 the vector of the solution of this problem $\vec{C}_M$ will be proportional to the vector $\vec{\zeta}^{(m_0)}(\vec{r}_0)$:

$$\vec{C}_M = C_0 e^{i\alpha}\frac{\vec{\zeta}^{(m_0)}(\vec{r}_0)}{\left|\vec{\zeta}^{(m_0)}(\vec{r}_0)\right|} \equiv \vec{C}_{\mathrm{mod}\, m_0}. \quad (9)$$

Here α is the arbitrary real number. If the set M contains several numbers, the vector $\vec{C}_M$ in the general case is not proportional to the vectors $\vec{\zeta}^{(m)}(\vec{r}_0)$ for the modes entering M. In this case, as well as in the case of radiator deflections in the horizontal planes when mutual orthogonality of the vectors $\vec{\zeta}^{(j)}(\vec{r}_0)$ is broken, the vector $\vec{C}_M$ can intensively excite parasitic modes as well.

The *L*-problem (7) on the maximal suppression of parasitic modes at the point $\vec{r}_0$. Let us denote its solution as $\vec{C}_L$. If the set L contains the number of the only mode l_0, any vector $\vec{C}_L$ (in addition to a zero one) that is orthogonal to the mode vector $\vec{\zeta}^{(l_0)}(\vec{r}_0)$ will serve as a solution and the corresponding optimal value of the functional will be $W_L(\vec{C}_L) = 0$. If L contains several numbers, the optimal vector $\vec{C}_L$ in the general case is not orthogonal to the vectors $\vec{\zeta}^{(l)}(\vec{r}_0)$ of the modes entering L and $W_L(\vec{C}_L) > 0 > 0$. Since useful modes do not participate in the statement of the L-problem, their intensities in the general case is not the maximum possible one. In particular, it is knowingly lower than that in the M-problem.

The *ML*-problem (8) of distinguishing of useful modes against the background of parasitic ones belong to the optimization problems since the functional $\{W_M, W_L\}$, which is to be optimized in it, is two-dimensional. We will call the vector $\vec{C}$ an unimprovable Pareto-solution (US) of the problem [11] if there is no excitation vector $\vec{C}_1$ that simultaneously increases the intensities of useful modes in the case of a nonincreasing intensities of the parasitic modes or which increases the latter in case of a nondecreasing useful mode, i.e., for which the following set of inequalities holds:

$$\begin{cases} W_M(\vec{C}_1) > W_M(\vec{C}) \\ W_L(\vec{C}_1) \le W_L(\vec{C}) \end{cases} \text{ or } \begin{cases} W_M(\vec{C}_1) \ge W_M(\vec{C}) \\ W_L(\vec{C}_1) < W_L(\vec{C}) \end{cases}.$$

In the general case, the set of all USs to problem (8) is infinite. Let $\vec{C}$ be an arbitrary US. It is clear that $W_M(\vec{C}) \le W_M(\vec{C}_M)$, $W_L(\vec{C}) \ge W_L(\vec{C}_L)$.. Taking this into account, let us introduce the vector $\vec{\gamma}(\vec{C}) = (\gamma_M, \gamma_L)$ characterizing the quality of a US with the components

$$\gamma_M(\vec{C}) = \frac{W_M(\vec{C})}{W_M(\vec{C}_M)}, \quad \gamma_L(\vec{C}) = \frac{W_L(\vec{C}_L)}{W_L(\vec{C})}, \tag{10}$$

and the scalar (defect)

$$\nu(\vec{C}) = 1 - \frac{\gamma_M(\vec{C}) + \gamma_L(\vec{C})}{2}. \tag{11}$$

Each of the introduced parameters (10) and (11) takes on values at the section [0, 1]. For example, $\vec{\gamma}(\vec{C}) = (0.9, 0.8)$ (defect $\nu = 0.15$) means that the intensity of useful modes $W_M(\vec{C})$ for this excitation vector $\vec{C}$ is 90% of the maximum possible one $W_M(\vec{C}_M)$, and the intensity of interfering modes $W_L(\vec{C})$ is $100/0.8 = 125\%$ of the minimum possible one $W_L(\vec{C}_L)$. The closer both components of the vector $\vec{\gamma}$ to 1, the higher the quality of the solution and the smaller the total defect ν. However, there can be no solution with a zero defect though the solution with a minimal defect usually exists.

It is clear that the characteristics of (10) and (11) can be calculated not only for US but also for an arbitrary excitation vector $\vec{C}$. The existing set Γ of all points $\vec{\gamma}(\vec{C})$ on the plane $((\gamma_L, \gamma_M))$ is a subset of the square $[0,1]\times[0,1]$. The boundary points of Γ (marked with a bold line in Fig. 1) for which displacements in the direction of growth of any of the coordinate deduces from the set Γ are the only ones that correspond to the unimprovable solutions; moreover, a US

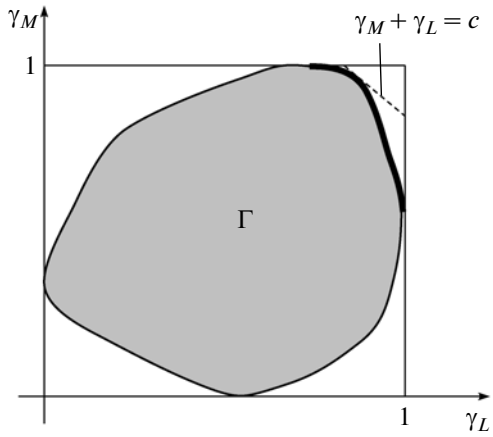

Fig. 1. Set of all possible values of the vector $\vec{\gamma} = (\gamma_L, \gamma_M)$.

with a minimal defect lies at the line of the level $\gamma_M + \gamma_L = c$ with a maximum possible value of the constant c (a dashed line in Fig. 1). Different USs for problem (8) can be found using extremum problems with the scalar functional associated with it. Consider examples of such problems.

Ratio-functional

$$J(\vec{C}) \equiv \frac{W_M(\vec{C})}{W_L(\vec{C})} \to \max_{\vec{C}\in\text{£}}. \tag{12}$$

The main drawback of such a functional and the USs to problem (8) associated with it is attributed to the fact that the maximum of $J(\vec{C})$ can be reached at small absolute values of the numerator owing to even smaller values of the denominator (in Fig. 1 these USs are observed in the lower part of a bold curve, where $\gamma_M \ll 1$). When this method of antenna array excitation is used, its resistance to radiation is mainly represented by a reactive component and the antenna weakly excites not only interfering, but also useful, modes (a superdirective antenna).

Difference-functional

$$J_\beta(\vec{C}) \equiv W_M(\vec{C}) - \beta W_L(\vec{C}) \to \max_{\vec{C}\in\text{£}}. \tag{13}$$

A nonnegative number β is an example of the functional. In particular, at $\beta = 0$ problem (13) transforms to (6) or to (7) at $\beta \to +\infty$ and the case of $\beta = 1$ corresponds to the difference of intensities of useful and parasitic modes. With an increase in β, the optimal value of the functional $J_\beta(\vec{C}_\beta)$ decreases and at some value of $\overline{\beta}$ vanishes. This $\overline{\beta}$ value coincides with the optimal functional in problem (12), and a corresponding vector $\vec{C}_{\overline{\beta}}$ simultaneously solves problem (12)

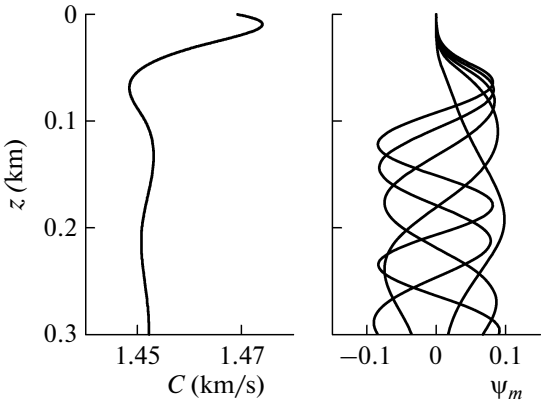

Fig. 2. The left plot: sound propagation velocity in a shallow sea (a summer profile). The right plot: profiles of the first five modes.

(A.6.4). It yields the following equivalent statement of problem (12):

$$\max_{\vec{C}\in\mathfrak{L}}\left|J_\beta\left(\vec{C}\right)\right| \to \min_\beta. \tag{14}$$

The quality of the solution $\vec{C}_\beta$ to problem (13) and its defect depend on β : $\vec{\gamma} = \vec{\gamma}\left(\vec{C}_\beta\right)$, $\nu = \nu\left(\vec{C}_\beta\right)$. This can be used when selecting the parameter β. For example, the value at which the defect of the problem solution $\nu\left(\vec{C}_\beta\right)$ is minimal can be taken as β. It yields the following version of the problem statement:

$$\begin{cases} J_\beta\left(\vec{C}_\beta\right) = \max\limits_{\vec{C}\in\mathfrak{L}} J_\beta\left(\vec{C}\right), \\ \nu\left(\vec{C}_\beta\right) \to \min\limits_\beta. \end{cases} \tag{15}$$

Problem (13) can be considered as a result of regularization of the L-problem when additional limitations are imposed on the reactive resistance of the antenna or on the total intensity of all modes [14]. For this, a stabilizer $\Omega\left(\vec{C}\right)$ is introduced and problem (7) is substituted by the problem $W_L\left(\vec{C}\right) - \varepsilon\Omega\left(\vec{C}\right) \to \min\limits_{\vec{C}\in\mathfrak{L}}$.. In particular, when selecting the intensity of useful modes $\Omega\left(\vec{C}\right) = W_M\left(\vec{C}\right)$ as a stabilizer, we get problem (13) with $\varepsilon = \beta^{-1}$.

Problems with limitations

Since it is useless to minimize the total level of parasitic modes below the level of additive waveguide noises, the only alternative to (8) is the following problem:

$$\begin{cases} W_M\left(\vec{C}\right) \to \max\limits_{\vec{C}\in\mathfrak{L}}, \\ W_L\left(\vec{C}\right) \le W_0, \end{cases} \tag{16}$$

where the problem parameter W_0 is determined by the intensity of additive noises. Problem (16) can be approximately solved, e.g., by using the penalty method [12] by maximizing the auxiliary functional $W_M\left(\vec{C}\right) - g\left(W_L\left(\vec{C}\right), W_0\right)$,, where $g\left(W_L\left(\vec{C}\right), W_0\right)$ is the penalty for violation of the inequality $W_L\left(\vec{C}\right) \le W_0$. The function $g_\alpha(x, W) = \{\alpha(x - W)^2$ where $\alpha > 0 > 0$ is the constant determining the rate of the penalty growth, can be taken, for example, as a penalty function.

4. NUMERICAL SIMULATION

When numerically solving the problems set forward in the previous section, we will use an observation typical for the Barents Sea. Consider a channel with a homogeneous path with the depth $H = 0.3$ km, a two-layer absorbing bottom, and an underlying half-space. The characteristics of the first bottom layer are as follows: the thickness is 0.005 km, the velocity of longitudinal waves is 1.430 km/s, the density is 1.6 g/cm^3, and the coefficient of attenuation of longitudinal waves is 0.05 dB/(km Hz). The characteristics of the second later are as follows: the thickness is 25 m, the velocity of longitudinal waves is 1.520 km/s, and the attenuation coefficient is 0.08 dB/(km Hz). The velocity of longitudinal waves in the underlying half-space is 2.5 km/s, the density is 2.2 g/cm^3, and the attenuation coefficient is 0.08 dB/(km Hz). The channel hydrology for the summer observation conditions is demonstrated in Fig. 2. It also shows the plots of the first five modes for the frequency $f_0 = 200$ Hz. The antenna radiators are positioned at the waveguide height every half wavelength apart, $d = \lambda_0/2 = 3.75$ m. In horizontal planes, some antenna elements can regularly and randomly be deflected from their initial positions owing to underwater flows. Antennas with different sizes will be used in the experiments, namely, a long antenna ($K = 60$, $\tilde{l}; 0.75$), a medium-size antenna ($K = 30$, $\tilde{l}; 0.37$), and a short antenna ($K = 15$, $\tilde{l}; 0.18$). Here $\tilde{l} = (K-1)d/H$ is the relative (with respect to the channel depth) length of the antenna. Here and hereinafter, the level $z_{\max}$ of the upper antenna radiator will be considered as the depth of the antenna immersion. The observation points will be taken at different depths at the horizontal distance from the antenna $r_0 = 10$ km.

To evaluate the quality of the proposed solution $\vec{C}$ to problem (8), in addition to calculation of the vector $\vec{\gamma}\left(\vec{C}\right)$ and the ratio $J\left(\vec{C}\right)$, we will compare it with a widely used mode method of antenna excitation when the vector of excitation coefficients is proportional to the profile of one of the useful modes: $\left(\vec{C}_{\mathrm{mod}\, m_0}\right)_k \sim \psi_{m_0}(z_k)$, $m_0 \in M$.. For that, we calculate

the ratio of the mode intensities corresponding to the compared vectors of antenna excitations:

$$r_M(\vec{C}) = \frac{W_M(\vec{C})}{W_M(\vec{C}_{\mathrm{mod}\,m_0})}, \quad r_L(\vec{C}) = \frac{W_L(\vec{C})}{W_L(\vec{C}_{\mathrm{mod}\,m_0})}. \quad (17)$$

If the vector $\vec{\gamma}(\vec{C})$ is an absolute characteristic of the vector $\vec{C}$ performing its comparison with all possible ways of antenna excitation, the vector $\vec{r}(\vec{C})$ is only a relative characteristic that compares $\vec{C}$ with a concrete vector $\vec{C}_{\mathrm{mod}\,m_0}$. The coefficient r_L does not usually exceed 1 for any US. In problems with only one useful mode, i.e., at $M = \{m_0\}$ and in the case of a vertical antenna, the coefficient r_M does not also exceed 1 and, at that, $r_M = \gamma_M$. If the set M contains more than one element or its individual radiators diverge from the vertical axis the, as a rule, $r_M \geq 1$, since in the case of the mode method of excitation only the intensity of the mode m_0 turns out to be high, whereas all other modes are weakly excited owing to their approximate orthogonality at the antenna array aperture.

Note that the field is often optimized at the expense of losses in the useful mode intensity (as compared to the mode method of excitation). This loss can, in principle, be compensated by a corresponding increase in the total power of the sources getting, as a result, the field with the same intensity of useful modes, the intensity of parasitic modes being lower.

The parameters of different USs are listed in Tables 1–11. The lower rows of the tables give the level of the observation point, and the captions show the dimensions and the depths of the antennas. The first rows of the tables list the type of excitation (the mode vector, the solution of M- or L-problems or that of problem (13), respectively). The values of the comparison parameters r_M, r_L, and J obtained for a given type of excitation are listed in a corresponding row of the tables.

4.1. Optimization of a Vertical Antenna

4.1.1. Distinguishing of mode 1. Consider the problem of distinguishing useful mode 1 against the background of parasitic modes with numbers 2–9, i.e., problem (8) for $M = \{1\}$, $L = \{2\text{–}9\}$. Let is position the observation points at the levels $z_0^{(1)} = 0.05$ km, $z_0^{(2)} = 0.19$ km. The first of these levels was close to the zero of the amplitude (node) of mode 1; the second one, to its extremum (antinode) (see scheme in Fig. 3). Since there is only one useful mode in this case, the solution of the M-problem coincides with mode 1: $\vec{C}_M = \vec{C}_{\mathrm{mod}1}$. Let us position the antennas in a waveguide so that their midpoints are near the antinode of mode 1 (the corresponding antenna depths

Table 1. Distinguishing of mode 1. A long antenna, depth 0.05 km

	r_M	r_L	J		r_M	r_L	J
$\vec{C}_M$	1	1	3.3	$\vec{C}_M$	1	1	397
$\vec{C}_1$	0.9	0.2	15.4	$\vec{C}_{30}$	0.99	0.43	919
$\vec{C}_3$	0.8	0.04	70.5	$\vec{C}_{90}$	0.96	0.22	1698
		...				...	
$\vec{C}_L$	0.76	2×10^{-15}	10^{15}	$\vec{C}_L$	0.76	2×10^{-14}	10^{16}
	$z_0^{(1)} = 0.05$ km				$z_0^{(2)} = 0.19$ km		

Table 2. Distinguishing of mode 1. A medium-size antenna, depth 0.12 km

	r_M	r_L	J		r_M	r_L	J
$\vec{C}_M$	1	1	0.23	$\vec{C}_M$	1	1	17
$\vec{C}_{0.2}$	0.9	0.6	0.34	$\vec{C}_{11}$	0.9	0.6	26
$\vec{C}_{0.4}$	0.2	0.1	0.5	$\vec{C}_{19}$	0.7	0.4	32
		...				...	
$\vec{C}_L$	2×10^{-5}	10^{-5}	0.3	$\vec{C}_L$	10^{-3}	5×10^{-3}	3.6
	$z_0^{(1)} = 0.05$ km				$z_0^{(2)} = 0.19$ km		

Table 3. Distinguishing of mode 1. A short antenna, depth 0.15 km

	r_M	r_L	J		r_M	r_L	J
$\vec{C}_M$	1	1	0.05	$\vec{C}_M$	1	1	4.6
$\vec{C}_{0.04}$	0.8	0.5	0.07	$\vec{C}_{3.6}$	0.8	0.6	6.2
$\vec{C}_{0.08}$	0.4	0.2	0.09	$\vec{C}_{5.6}$	0.5	0.3	8.1
		...				...	
$\vec{C}_L$	6×10^{-6}	8×10^{-6}	0.04	$\vec{C}_L$	4×10^{-4}	10^{-4}	13
	$z_0^{(1)} = 0.05$ km				$z_0^{(2)} = 0.19$ km		

Table 4. Distinguishing of mode 3. A long antenna, depth 0.05 km

	r_M	r_L	J		r_M	r_L	J
$\vec{C}_M$	1	1	16	$\vec{C}_M$	1	1	10.6
$\vec{C}_1$	0.99	0.67	23	$\vec{C}_1$	0.98	0.47	22
$\vec{C}_{11}$	0.85	0.15	90	$\vec{C}_{11}$	0.87	0.1	91
		...				...	
$\vec{C}_L$	0.24	2×10^{-15}	10^{15}	$\vec{C}_L$	0.22	6×10^{-5}	4×10^4
	$z_0^{(1)} = 0.08$ km				$z_0^{(2)} = 0.18$ km		

Table 5. Distinguishing of mode 3. A medium-size antenna, depth 0.05 km

	r_M	r_L	J		r_M	r_L	J
$\vec{C}_M$	1	1	2.0	$\vec{C}_M$	1	1	6.2
$\vec{C}_{0.1}$	0.99	0.92	2.2	$\vec{C}_1$	0.97	0.58	10
$\vec{C}_{3.1}$	0.73	0.44	3.4	$\vec{C}_7$	0.85	0.29	18
	...				...		
$\vec{C}_L$	3×10^{-3}	5×10^{-2}	0.1	$\vec{C}_L$	7×10^{-5}	10^{-2}	0.04
	$z_0^{(1)} = 0.08$ km				$z_0^{(2)} = 0.18$ km		

Table 6. Distinguishing of mode 3. A short antenna, depth 0.05 km

	r_M	r_L	J		r_M	r_L	J
$\vec{C}_M$	1	1	1.74	$\vec{C}_M$	1	1	1.66
$\vec{C}_{0.4}$	0.99	0.91	1.89	$\vec{C}_{0.5}$	0.99	0.92	1.77
$\vec{C}_2$	0.83	0.66	2.18	$\vec{C}_{1.5}$	0.87	0.73	1.97
	...				...		
$\vec{C}_L$	2×10^{-5}	2×10^{-3}	0.02	$\vec{C}_L$	2×10^{-6}	10^{-4}	0.03
	$z_0^{(1)} = 0.08$ km				$z_0^{(2)} = 0.18$ km		

Table 7. Distinguishing of modes 2 and 3. A long antenna, depth 0.05 km

	r_M	r_L	J		r_M	r_L	J
$\vec{C}_{\mathrm{mod}3}$	1	1	19	$\vec{C}_{\mathrm{mod}3}$	1	1	10.7
$\vec{C}_M$	1.21	0.06	379	$\vec{C}_M$	1.0	1.0	10.7
$\vec{C}_1$	1.21	0.03	787	$\vec{C}_1$	0.98	0.47	22
$\vec{C}_{11}$	1.20	0.002	10^4	$\vec{C}_{11}$	0.97	0.1	96
	...				...		
$\vec{C}_L$	0.99	2×10^{-15}	3×10^{16}	$\vec{C}_L$	0.4	4×10^{-15}	1×10^{15}
	$z_0^{(1)} = 0.08$ km				$z_0^{(2)} = 0.18$ km		

Table 8. Distinguishing of modes 2 and 3. A medium-size antenna, depth 0.05 km

	r_M	r_L	J		r_M	r_L	J
$\vec{C}_{\mathrm{mod}3}$	1	1	3.9	$\vec{C}_{\mathrm{mod}3}$	1	1	6.35
$\vec{C}_M$	1.3	0.26	20	$\vec{C}_M$	1.	1.	6.33
$\vec{C}_1$	1.3	0.22	23	$\vec{C}_1$	0.97	0.58	10.6
$\vec{C}_{11}$	1.29	0.19	26	$\vec{C}_{11}$	0.79	0.25	20.4
	...				...		
$\vec{C}_L$	3×10^{-5}	10^{-5}	11	$\vec{C}_L$	2×10^{-4}	0.01	0.09
	$z_0^{(1)} = 0.08$ km				$z_0^{(2)} = 0.18$ km		

are 0.05 km for a long antenna, 0.12 km for a medium-size antenna, and 0.15 km for a short antenna). The results of the solution of different optimization problems for the described configurations are listed in Tables 1–3.

As is apparent from Table 1, owing to optimization in the case of a long antenna, it is possible to substantially lower the intensity of parasitic modes at a slight decrease in the parasitic mode intensities and drastically increase the ratio of J. This is valid within a wide range of observation point depths, but the case in which the observation point is far from the antinode of the useful mode where the relative intensity of parasitic modes during the mode method of excitation can be rather high (the left one in Table 1) is of particular interest. In case of a long antenna, both the solutions to $\vec{C}_\beta$ obtained from problem (13) with specially selected values of β and the solutions to the problem $\vec{C}_L$ (Fig. 4) are of interest from the practical point of view. High controllability of the antenna is attributed to the fact that the condition of orthogonality of different modes with respect to one another is well-met on its aperture. The optimal solutions present themselves as variations of the mode solution $\vec{C}_{\mathrm{mod}1}$ (Fig. 5). Since a long antenna occupies the greater part of the vertical waveguide cross section, the position of its center does not actually affect the optimization quality.

With shortening of the antenna, an excess of the intensities of useful modes over parasitic ones for the mode method of excitation rapidly decreases, which is related to the brake of mode orthogonality properties on the antenna aperture. Objectively, this creates interest in performing optimization. Unfortunately, the calculations show that the possibilities of optimization also rapidly decrease with a decrease in the number of radiators. Thus, in the case of a medium-size and short antennas (Tables 2, 3), we managed to increase the ratio J only by 30–80% as compared to the mode method of excitation, 20–30% of the useful mode intensity being lost. The solution $\vec{C}_L$ for short

Table 9. Distinguishing of modes 2 and 3. A short antenna, depth 0.05 km

	r_M	r_L	J		r_M	r_L	J
$\vec{C}_{\mathrm{mod}3}$	1	1	3.3	$\vec{C}_{\mathrm{mod}3}$	1	1	1.67
$\vec{C}_M$	1.01	0.95	3.5	$\vec{C}_M$	1.	1.	1.67
$\vec{C}_1$	0.98	0.78	4.1	$\vec{C}_1$	0.95	0.83	1.9
$\vec{C}_3$	0.82	0.51	5.4	$\vec{C}_{1.5}$	0.87	0.73	1.99
	...				...		
$\vec{C}_L$	3×10^{-5}	10^{-5}	9	$\vec{C}_L$	2×10^{-6}	10^{-4}	0.03
	$z_0^{(1)} = 0.08$ km				$z_0^{(2)} = 0.18$ km		

antennas is, as a rule, of no practical interest (even when the maximum value of the ratio J is reached), since the intensity of a useful mode in this case makes only a small fraction of the intensity implemented during mode excitation. At small antenna sizes, the efficiency of optimization, in addition, depends on the antenna position in a waveguide.

4.1.2. Distinguishing of mode 3. Consider the problem of distinguishing useful mode 3 against the background of parasitic modes with numbers 1–2, 4–9, i.e., problem (8) for $M = \{3\}$, $L = \{1–2, 4–9\}$. Contrary to the problem solved in Section 4.1.1, useful mode 3 in a waveguide has three intensity levels and we can trace in detail the dependence of the optimization efficiency on the mutual positioning of the antenna and the observation points. Let us position the latter at the levels $z_0^{(1)} = 0.08$ and $z_0^{(2)} = 0.18$ km and place the antennas at the depth of 0.05 km near the upper antinode of mode 3 (Fig. 6). As in the previous case, the most useful mode ($m_0 = 3$) is chosen as a reference mode. The solution of the M-problem also coincides here with the mode one, $\vec{C}_{\text{mod}3}$.

The versions of the solution to the considered problem for the antennas with different lengths are listed in Tables 4–6. It is apparent from Table 4 that, in the case of a long antenna that covers the entire waveguide, the quality of optimization does not actually depend on the position of the observation point. For a medium-size antenna asymmetrically positioned in a waveguide with respect to the useful mode antinodes, the parasitic modes at the low observation points are suppressed more effectively as compared to that at the upper point. In the case of a short antenna, the optimization effect is negligible in the entire waveguide space.

4.1.3. Distinguishing of modes 2, 3. Consider now the problem of distinguishing useful modes with numbers $M = \{2,3\}$ against the background of parasitic modes with the numbers $L = \{1, 4–9\}$. The observation points were the same as those in the previous problem at the levels $z_0^{(1)} = 0.08$ and $z_0^{(2)} = 0.18$ km far to the antinodes of mode 3 (Fig. 7). The first level also corresponded to the antinode of mode 2; the second one, to the node of mode 2 and the antinode of mode 3. The mode $m_0 = 3$ was chosen as a reference mode. Since now the solution $\vec{C}_M$ does not coincide, in the general case, with the mode vector $\vec{C}_{\text{mod}3}$ an additional row characterizing the mode method of excitation is added to the table.

When solving the problem with many useful modes, an evident drawback of the mode method of excitation is attributed to the fact that only one mode is efficiently excited in it, namely, the mode m_0, whereas all other modes (both useful and parasitic) are poorly excited on the antenna aperture owing to their mutual orthogonality. When optimal methods of excitation are applied, a certain compromise is reached when all useful modes are excited to a sufficient degree, although the intensities of different useful modes are different (Figs. 8–10). However, these intensities can be equalized during optimization using the functional the intensities of different modes enter with different weights instead of Eq. (5).

Table 10. Distinguishing of mode 1. The problem with randomly oscillating radiators. A long antenna, depth 0.05 km

$\delta r = 0.001$ km

	r_M	r_L	J		r_M	r_L	J
$\vec{C}_{\text{mod}1}$	1	1	2.65	$\vec{C}_{\text{mod}1}$	1	1	216
$\vec{C}_M$	1.07	0.87	3.26	$\vec{C}_M$	1.06	0.58	397
$\vec{C}_1$	0.99	0.17	15.4	$\vec{C}_{30}$	1.05	0.25	919
$\vec{C}_3$	0.91	0.03	70.5	$\vec{C}_{90}$	1.02	0.13	1698
		...				...	
$\vec{C}_L$	0.75	10^{15}	2×10^{15}	$\vec{C}_L$	0.76	6×10^{-16}	2×10^{17}
	$z_0^{(1)} = 0.05$ km				$z_0^{(2)} = 0.19$ km		

$\delta r = 0.002$ km

	r_M	r_L	J		r_M	r_L	J
$\vec{C}_{\text{mod}1}$	1	1	1.03	$\vec{C}_{\text{mod}1}$	1	1	106
$\vec{C}_M$	1.3	0.41	3.26	$\vec{C}_M$	1.25	0.33	397
$\vec{C}_1$	1.19	0.08	15.4	$\vec{C}_{30}$	1.24	0.14	919
$\vec{C}_3$	1.09	0.02	70.5	$\vec{C}_{90}$	1.20	0.07	1698
		...				...	
$\vec{C}_L$	0.74	3×10^{-15}	2×10^{15}	$\vec{C}_L$	0.76	6×10^{-16}	2×10^{17}
	$z_0^{(1)} = 0.05$ km				$z_0^{(2)} = 0.19$ km		

Table 11. Distinguishing of mode 1. The problem with an inclined antenna array. A long antenna, depth 0.05 km

$\alpha = \pi/4$, $\delta r = 0.002$ km

	r_M	r_L	J		r_M	r_L	J
$\vec{C}_{\text{mod}1}$	1	1	0.14	$\vec{C}_{\text{mod}1}$	1	1	15.8
$\vec{C}_M$	1.5	0.07	3.26	$\vec{C}_M$	1.5	0.06	397
$\vec{C}_1$	1.4	0.01	15.4	$\vec{C}_{30}$	1.5	0.03	919
$\vec{C}_3$	1.28	0.002	70.5	$\vec{C}_{90}$	1.46	0.01	1698
		...				...	
$\vec{C}_L$	1.16	4×10^{-16}	3×10^{14}	$\vec{C}_L$	0.16	10^{-15}	10^{16}
	$z_0^{(1)} = 0.05$ km				$z_0^{(2)} = 0.19$ km		

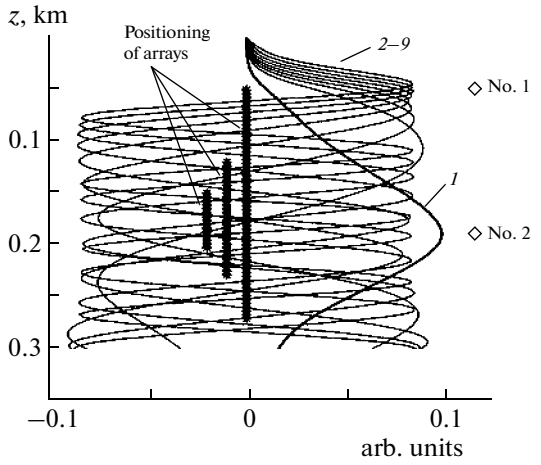

Fig. 3. A scheme of positioning of antennas and observation points over the waveguide depth in the problem of distinguishing mode 1 against the background of modes 2–9. Asterisks mark the positions of the radiators for three types of antennas, rhombs mark the observation points: no. 1—$z_0^{(1)} = 0.05$ km, no. 2—$z_0^{(2)} = 0.19$ km. Contrary to parasitic modes, useful mode 1 is marked with a bold line.

The results of the simulation of the considered problem are demonstrated in Tables 7–9. Comparing the obtained data with the analogous ones given in Sections 4.1.1 and 4.1.2, we can come to the conclusion that, in the case of many useful modes, optimization is more efficient. The reason is as follows: in this case, for any observation point, there is a useful mode the antinode of which is near this point. Consequently, intensification of the total intensity of useful modes during optimization takes place owing to this mode. For example, the optimal vectors for the observation point $z_0^{(1)}$ are close to the vector $\vec{C}_{\mathrm{mod}\,2}$ (Fig. 9); those for the point $z_0^{(2)}$, to the vector $\vec{C}_{\mathrm{mod}\,3}$ (Fig. 11).

4.2. Optimization of an Oscillating Antenna

Consider the problems of optimization of the mode composition of the field generated by a set of radiators deflecting in horizontal planes. Let us return to the problem from Section 4.1.1 on distinguishing of mode 1 against the background of all other modes, the problem parameters being the same (Fig. 3). It follows from Eq. (9) that, for deflecting radiators, the optimal solutions $\vec{C}_M$ even in case on one useful mode differ from the mode ones $\vec{C}_{\mathrm{mod}1}$. Thus, they are given in a separate row in the next tables.

4.2.1. Random deflections of radiators. Random deflections of individual radiators in a horizontal plane will be simulated in the form $x_k = (\xi_k - 1/2)\delta r$, $y_k = (\eta_k - 1/2)\delta r$, where $\{\xi_k,\ \eta_k,\ k = 1...K\}$ are the independent random quantities uniformly distributed at the section [0, 1], and δr is the parameter determining dispersion (a standard) of radiator deflections. In this case, the mode intensities and optimal excitation vectors depend of the radiator deflections and, thus, they are random as well. This is why the values listed in Table 10 should be considered as selected ones that correspond to the given realizations of radiator deflections. In particular, the ratios J in the case of a mode excitation method and the coefficients r_M, r_L for the optimal solutions

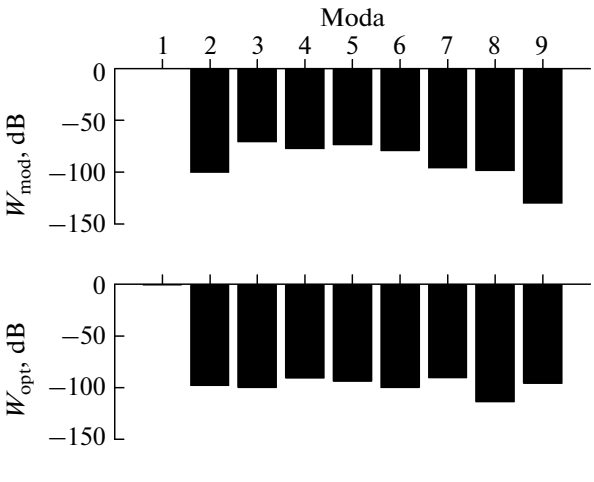

Fig. 4. Intensities (dB) of modes during mode $\vec{C}_{\mathrm{mod}1}$ (the upper plot) and optimal $\vec{C}_{90}$ (the lower plot) methods of antenna excitation. A long antenna, depth 0.05 km, the observation point is $z_0^{(1)} = 0.05$ km (the left one in Table 1).

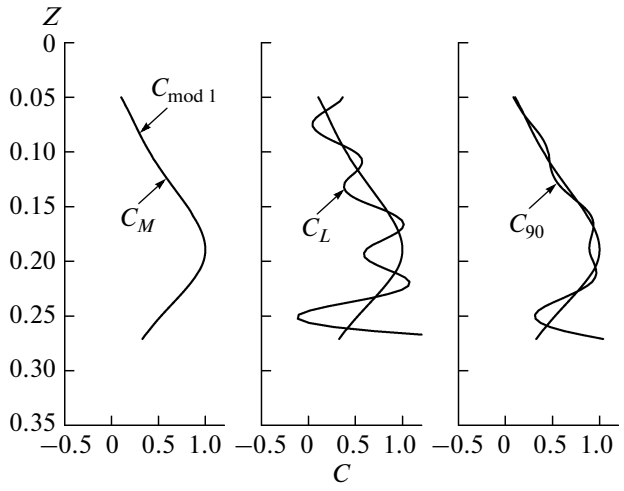

Fig. 5. Solutions to the problem of distinguishing mode 1 against the background of modes 2–9 normalized by $\max \vec{C}_M$. From left to right: $\vec{C}_M$, $\vec{C}_L$, $\vec{C}_{90}$. A long antenna, depth 0.05 km, the observation point is $z_0^{(2)} = 0.19$ km (the right one in Table 1).

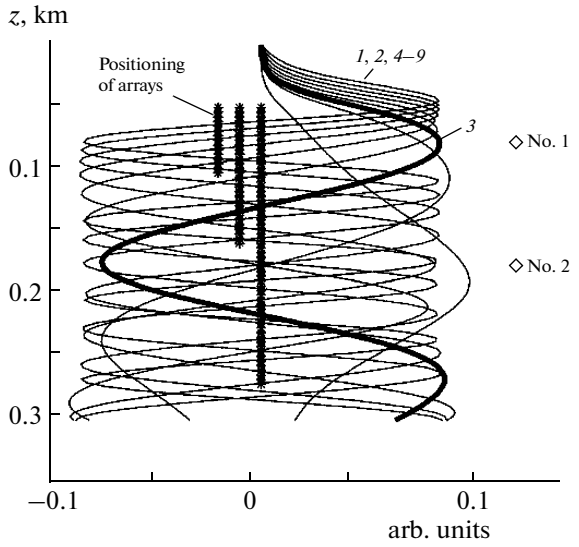

Fig. 6. A scheme of positioning of observation points in the problem of distinguishing mode 3 against the background of modes 1, 2 and 4–9 (Section 3.1). Asterisks mark the positions of the radiators, rhombs mark the observation points: no. 1—$z_0^{(1)} = 0.08$ km, no. 2—$z_0^{(2)} = 0.18$ km. Contrary to parasitic modes, useful mode 3 is marked with a bold line.

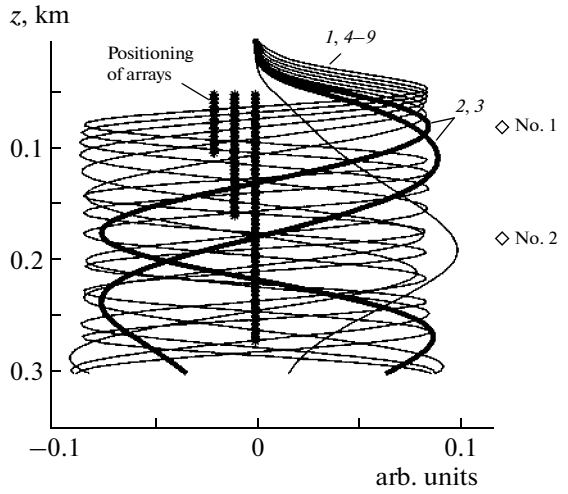

Fig. 7. A scheme of positioning of antennas and observation points in the problem of distinguishing modes 2 and 3 against the background of modes 1 and 4–9. Asterisks mark the positions of the radiators; rhombs mark the observation points: no. 1—$z_0^{(1)} = 0.08$ km, no. 2—$z_0^{(2)} = 0.18$ km. Contrary to parasitic modes, useful modes 2 and 3 are marked with bold lines.

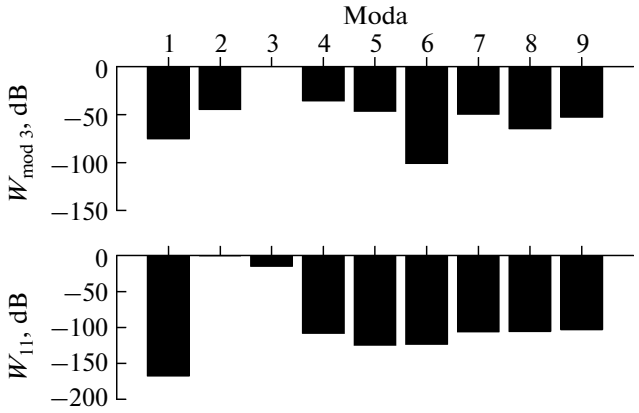

Fig. 8. The problem of distinguishing modes 2 and 3 against the background of modes 1 and 4–9. The intensities (dB) of modes during mode $\vec{C}_{\text{mod}3}$ (the upper plot) and optimal $\vec{C}_{11}$ (the lower plot) methods of antenna excitation. A long antenna, depth 0.05 km, the observation point is $z_0^{(1)} = 0.08$ km (the left one in Table 7).

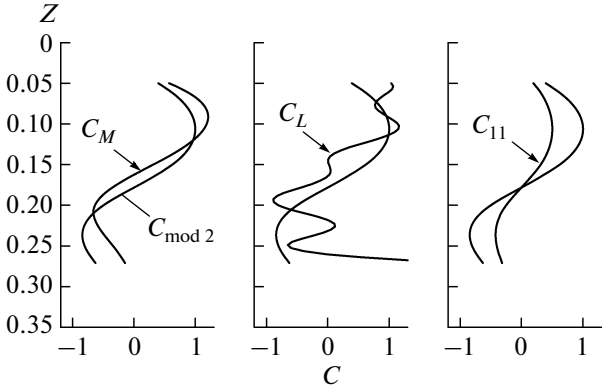

Fig. 9. Solutions to the problem of distinguishing modes 2 and 3 against the background of modes 1 and 4–9: $\vec{C}_M, \vec{C}_L, \vec{C}_{11}$ (from left to right). A long antenna, depth 0.05 km, the observation point is $z_0^{(1)} = 0.08$ km (the left one in Table 7).

are random. Moreover, the power ratios J for the optimal solutions are no longer optimal, are determined only by a type of the solution and do not depend on radiator deflections.

4.2.2. An inclined antenna. Regular deflections of antenna array radiators from the vertical axis are simulated as follows:

$$x_k = h_x k,\ y_k = h_y k,$$
$$h_x = -2x_1/(K-1), h_y = -2y_1/(K-1),$$
$$x_1 = \delta r \cos\alpha,\ y_1 = \delta r \sin\alpha.$$

Here $\alpha, \delta r$ are the parameters that determine the antenna inclination. The results of the solution of this problem are listed in Table 11. Comparison of

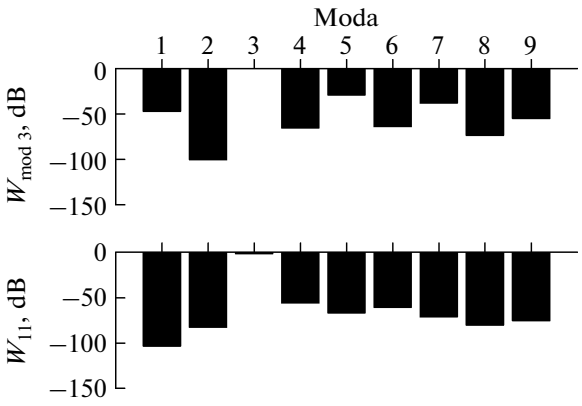

Fig. 10. Solutions to the problem of distinguishing modes 2 and 3 against the background of modes 1 and 4–9. Intensities (dB) of modes during mode $\vec{C}_{\text{mod}3}$ (the upper plot) and optimal $\vec{C}_{11}$ (the lower plot) methods of antenna excitation. A long antenna, depth 0.05 km, the observation point is $z_0^{(1)} = 0.18$ km (the right one in Table 7).

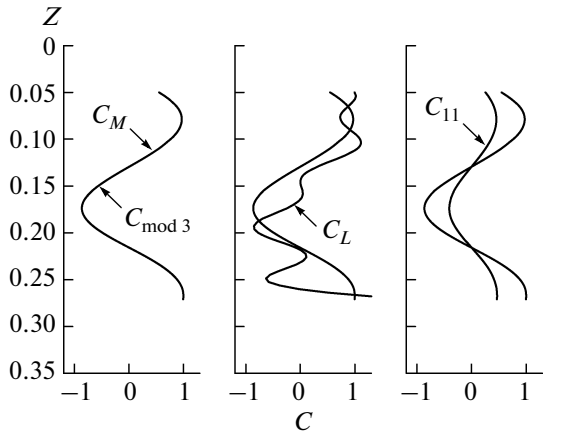

Fig. 11. Solutions to the problem of distinguishing modes 2 and 3 against the background of modes 1 and 4–9: $\vec{C}_M, \vec{C}_L, \vec{C}_{11}$ (from left to right). A long antenna, depth 0.05 km, the observation point is $z_0^{(1)} = 0.18$ km (the right one in Table 7).

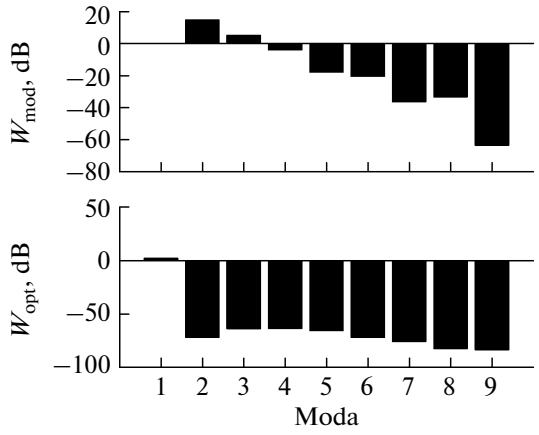

Fig. 12. Intensities of individual modes (dB) during mode $\vec{C}_{\text{mod}1}$ (the upper plot) and optimal $\vec{C}_3$ (the lower plot) methods of antenna excitation. A long inclined antenna, depth 0.05 km, the observation point is $z_0^{(1)} = 0.05$ km, the antenna inclination angle is $\alpha = \pi/4$, the standard of radiator deflections is $\delta r = 0.002$ km (the left one in Table 11).

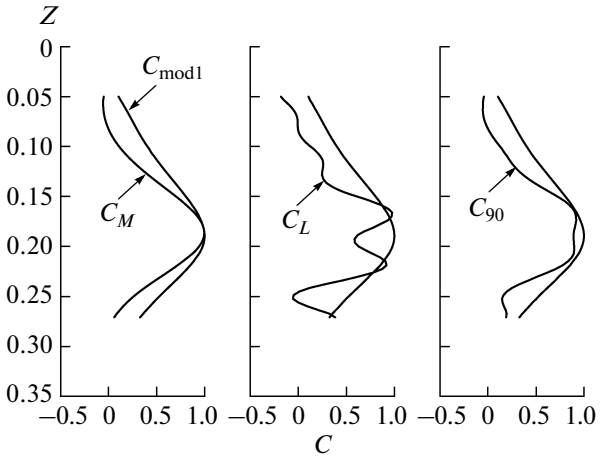

Fig. 13. Optimal solutions of different type. From left to right: $\text{Re}C_M, \text{Re}C_L, \text{Re}C_{90}$, and $\text{Re}C_{\text{mod}1}$ normalized by $\max C_{\text{mod}1}$. A long inclined antenna, depth 0.05 km, the observation point is $z_0^{(2)} = 0.19$ km, the antenna inclination angle is $\alpha = \pi/4$, the standard of radiator deflections is $\delta r = 0.002$ km (the right one in Table 11).

Tables 1, 10 and 11 shows that the parameters of mode tuning and the optimal solutions depend on the antenna inclination. Moreover, as in the previous problem, the ration of intensities of useful and interfering modes J for the optimal solutions are determined only by the solution type and do not depend on the antenna deflection (Figs. 12, 13).

CONCLUSIONS

The vectors $\vec{\zeta}^{(m,l)}(\vec{r}_0)$ for an inclined antenna depend on r_0 and on the deflection of individual radiators in the horizontal plane $\vec{\rho}_k$ (see Eq. (2)). As a result, the solutions to problems (6)–(16) also depend on these parameters: $\vec{C} = \vec{C}(\vec{r}_0, \{\vec{\rho}_k\})$. This means that for the optimal fields to be generated the radiator, excitation coefficients at different observation points should be chosen in a different manner and for the optimal field composition to be preserved it is necessary to adjust the tuning depending on the variations in the radiator positions. The last condition imposes a limitation of the rate of solution of the corresponding optimization problems: it is to be sufficiently high to provide for optimal tuning in real time.

The numerical solution of the problems of optimization of the mode composition of a field in a shallow-water oceanic waveguide set in Section 3 points to the fact that a number of factors affect the efficiency of optimization, i.e., a substantial increase in the ratio J of useful and parasitic mode during preservation of the useful mode level. First, these are the dimensions $\tilde{l}$ of the antenna array systems related to the waveguide depth (for the radiators positioned every half-wavelength). Second, this is the position of the observation point with respect to antinodes and nodes of useful modes. A general conclusion is as follows: optimization is effective near the antinodes of useful modes at $\tilde{l} > 0.3$.

In the case of a vertical antenna, optimal methods of excitation are usually inferior to the mode ones as far as intensities of useful modes W_M are concerned, but are superior in the intensity ratio $J = W_M/W_L$. As for inclined antennas, optimal excitations are usually superior to the mode ones in both parameters. In addition, contrary to the second ones vertical antennas are characterized by stable values of J at variations in the radiator positions.

ACKNOWLEDGMENTS

The study was supported by the Russian Foundation for Basic Research (project no. 09-02-00044); by the programs "Coherent Acoustic Fields and Signals" and "The Fundamental Basis of Acoustic Diagnostics of Artificial and Natural Media" of the OFN, Russian Academy of Sciences; by the Federal Target Program "Scientific and Scientific–Pedagogical Cadres of Innovative Russia" for 2009–2013 (contract no. 02.740.11.0565), and a grant for Russian Federation Presidential Program in Support of Leading Scientific Schools (NSh-3700.2010.2).

APPENDIX

This section gives a summary of the basic methods of a numerical solution of problems (12) and (13). Consider the problem

$$J_\beta(\vec{C}) = \sum_{m\in M}\left|\left\langle \vec{C},\vec{\zeta}^{(m)}\right\rangle\right|^2 - \beta\sum_{l\in L}\left|\left\langle \vec{C},\vec{\zeta}^{(l)}\right\rangle\right|^2 \to \max_{\vec{C}\in £}, \quad (18)$$

where M and L are the specified disjoint sets of mode indices. Assume that at some value of $\vec{C}$ the functional is positive. Then, with an increase in the norm of the vector $\vec{C}$, the functional only increases. Thus, the solution of the problem $\vec{C}_{\max}$ in this case has the maximum possible norm C_0. If the functional is not everywhere positive, the zero vector $\vec{C}_{\max} = 0$ at which the functional is zero is one of the solutions to the problem. Any methods described below in Sections A.1–A.3 can be used for solving problem (18). It follows from the results of Section A.4 that the solution to problem (12) can be reduced to the solution of the family of problems (13) over the parameter β.

A.1. The Method of Conditional Gradient Descent

Taking into account the simplicity of an analytical description of functionals (12) and (13), the methods of gradient descent can be applied for solving corresponding problems. For the gradient of the functional J_β over the complex-conjugate variable $\vec{C}^*$, we have the expression

$$\nabla_{\vec{C}^*}J_\beta(\vec{C}) = \sum_{m\in M}\left\langle \vec{C},\vec{\zeta}^{(m)}\right\rangle\vec{\zeta}^{(m)} - \beta\sum_{l\in L}\left\langle \vec{C},\vec{\zeta}^{(l)}\right\rangle\vec{\zeta}^{(l)}.$$

Since the variable $\vec{C}$ does not change in the entire space but only on a closed set £, the extremum should be sought for using the method of a conditional gradient [12]. A new approximation $\vec{C}_{k+1}$ is found from the old $\vec{C}_k$ according to the rule

$$\vec{C}_{k+1} = C_0\frac{\vec{C}_k + \lambda_k\vec{E}_k}{\left|\vec{C}_k + \lambda_k\vec{E}_k\right|}, \quad (19)$$

where $\vec{E}_k = \nabla_{\vec{C}^*}J_\beta(\vec{C}_k)/\left|\nabla_{\vec{C}^*}J_\beta(\vec{C}_k)\right|$ is the normalized value of the functional gradient at the point $\vec{C}_k$. The scalar $\lambda_k > 0$ is chosen from the condition

$$J_\beta(\vec{C}_{k+1}) > J_\beta(\vec{C}_k). \quad (20)$$

The initial step is $\lambda = \lambda_0$; then the step is fragmented until condition (20) is met. The convergence of sequence (19) to the problem solution and the convergence rate depend on how successfully the initial vector $\vec{C}_0$ and the initial step λ_0 are chosen.

A.2. The Rayleigh Method

Problem (18) is closely connected with the known classical problem from the spectral theory of matrices [13] on stationary values of the Rayleigh ratio. It is evident that in the theoretical analysis it is sufficient to restrict oneself to the case of $\beta = 1$. Let us write the functional $J_1(\vec{C})$ differently. Assuming $K = M \cup L$; $\gamma_m = 1$, $m \in M$; $\gamma_l = -1$, and $l \in L$, we have

$$J_1(\vec{C}) = \sum_{m\in K}\gamma_m\left|\left\langle \vec{C},\vec{\zeta}^{(m)}\right\rangle\right|^2 = \sum_{m\in K}\gamma_m\left|\sum_k C_k\zeta_k^{(m)}\right|^2$$
$$= \sum_{m\in K}\gamma_m\sum_k\sum_{k'}C_kC_{k'}^*\zeta_k^{(m)*}\zeta_{k'}^{(m)} = \left\langle \alpha\vec{C},\vec{C}\right\rangle,$$

where α is the Hermite matrix on the order of $K \times K$ with the components $\alpha_{k'k} = \sum_{m\in K}\gamma_m\zeta_{k'}^{(m)}\zeta_k^{(m)*}$. As a

result, we obtain the following representation of the functional

$$J_1(\vec{C}) = \langle \alpha\vec{C},\vec{C}\rangle = R_\alpha(\vec{C})\langle \vec{C},\vec{C}\rangle, \quad (21)$$

where $R_\alpha(\vec{C}) \equiv \langle \alpha\vec{C},\vec{C}\rangle / \langle \vec{C},\vec{C}\rangle$ is the Rayleigh ratio for the matrix α. If the functional maximum is positive, the solution of the problem is always reached at the boundary of the set £, where $\langle \vec{C},\vec{C}\rangle = |\vec{C}|^2 = C_0^2$, and, thus, owing to (21) the problem is equivalent to the following one:

$$R_\alpha(\vec{C}) \to \max_{|\vec{C}|=C_0}. \quad (22)$$

Hence, the solution to problem (18) can be obtained from the theory of problem (22). Let us give the main result of the latter. Let $\mu_{\max} > 0$ be the maximal eigenvalue of the Hermite matrix α and $\vec{C}_{\max}$ be the eigenvector with the norm $|\vec{C}_{\max}| = C_0$ corresponding to it. This vector is the solution to problem (22) and the corresponding value of the functional is $J_1(\vec{C}_{\max}) = \mu_{\max} C_0^2$.

A.3. The Lagrange Method

Considering the set of vectors $\{\vec{\zeta}^{(m)},\vec{\zeta}^{(l)} \mid m \in M, l \in L\}$ to be linearly independent, let us consider problem (18) for $\beta = 1$. Let us show that this solution is a linear combination of the vectors $\vec{\zeta}^{(k)}$. Let us construct the Lagrange function

$$L = \lambda_0\left\{\sum_{m\in M}\left|\langle \vec{C},\vec{\zeta}^{(m)}\rangle\right|^2 - \sum_{l\in L}\left|\langle \vec{C},\vec{\zeta}^{(l)}\rangle\right|^2\right\} + \lambda_1|\vec{C}|^2,$$

where λ_0, λ_1 are the Lagrange correlation coefficients (real numbers that are not simultaneously zero). For the vector $\vec{C}$ to be optimal, it is necessary for the Lagrange function gradient to be zero over the conjugate vector $\vec{C}^*$ (the Euler equation),

$$\nabla_{C^*}L = \lambda_0\left\{\sum_{m\in M}\langle \vec{C},\vec{\zeta}^{(m)}\rangle\vec{\zeta}^{(m)} - \sum_{l\in L}\langle \vec{C},\vec{\zeta}^{(l)}\rangle\vec{\zeta}^{(l)}\right\} + \lambda_1\vec{C} = 0, \quad (23)$$

from which follows the above statement.

Thus, the solution to Eq. (18) can be sought in the form

$$\vec{C}_{\max} = C_0\left\{\sum_{m\in M}x_m\vec{\zeta}^{(m)} + \sum_{l\in L}y_l\vec{\zeta}^{(l)}\right\}, \quad (24)$$

where $\{x_m, y_l \mid m \in M, l \in L\}$ are complex expansion coefficients normalized by the condition

$$\left|\sum_{m\in M}x_m\vec{\zeta}^{(m)} + \sum_{l\in L}y_l\vec{\zeta}^{(l)}\right| = 1. \quad (25)$$

Since $|\lambda_0| + |\lambda| > 0$ and $\vec{C} \neq 0$, we get from Eq. (23) that $\lambda_0 \neq 0$ and, thus, we can consider that $\lambda_0 = 1$. Then, from Eqs. (23) and (24) we have

$$\sum_{m\in M}\left(\langle \vec{C}_{\max},\vec{\zeta}^{(m)}\rangle + \lambda C_0 x_m\right)\vec{\zeta}^{(m)} + \sum_{l\in L}\left(-\langle \vec{C}_{\max},\vec{\zeta}^{(l)}\rangle + \lambda C_0 y_l\right)\vec{\zeta}^{(l)} = 0. \quad (26)$$

For a linearly independent set $\{\vec{\zeta}^{(m)},\vec{\zeta}^{(l)}\}$, all coefficients in zero vector expansion (26) are zero. Hence, after substitution of Eq. (24) into Eq. (26), we get a set of equations for the coefficients $\{x_m, y_l\}$

$$\begin{cases}\sum_{m'\in M}(s_{m'm} + \lambda\delta_{m'm})x_{m'} + \sum_{l'\in L}s_{l'm}y_{l'} = 0, & m \in M,\\ \sum_{m'\in M}s_{m'l}x_{m'} + \sum_{l'\in L}(s_{l'l} - \lambda\delta_{l'l})y_{l'} = 0, & l \in L,\end{cases} \quad (27)$$

where $s_{lm} \equiv \langle \vec{\zeta}^{(l)},\vec{\zeta}^{(m)}\rangle$. Introducing the coefficient vector $z = \{x_m, y_l\}$ and a corresponding matrix of the coefficients S, we write set of equations (27) in a matrix form

$$Sz = \lambda z, \quad (28)$$

hence, it follows that λ is the eigenvalue of the matrix S and z is the eigenvector that meets normalization condition (25). As follows from Eq. (26), the corresponding value of the functional has the form

$$J(\vec{C}_{\max}) = C_0^2\lambda^2\left(\sum_{m\in M}|x_m|^2 - \sum_{l\in L}|y_l|^2\right). \quad (29)$$

Thus, problem (18) is also reduced to the solution of spectral problem (25)–(28) and the selection of one of its solutions for which functional (29) is maximal.

A.4. Method of Reduction

This section shows how the problem of the maximum of the functional-ratio can be reduced to a family of more elementary problems for the difference-functionals. The method is based on the following statement proved in [15].

Lemma. Let $W(x) > 0, W_1(x)$ be the functionals continuous on a compact set K of the matrix space and β be a positive number

$$J(x) \equiv \frac{W_1(x)}{W(x)}, \quad J_\beta(x) \equiv W_1(x) - \beta W(x).$$

Let us consider the extremum problems

$$J \to \max_{K}, \tag{30}$$

$$J_\beta \to \max_{K}. \tag{31}$$

Let $x_{\max}$ be the solution to problem (30) and x_β be the solution to problem (31) $\beta_{\max} \equiv J(x_{\max}), j(\beta) \equiv J_\beta(x_\beta)$. Then

$$j(\beta) < 0, \quad \beta > \beta_{\max}; \quad j(\beta) > 0,$$
$$\beta < \beta_{\max}; \quad j(\beta) = 0, \quad \beta = \beta_{\max}$$

and, thus, $\beta_{\max}$ is the only solution to the equation $j(\beta) = 0$. The extrema of the functionals $J(x)$ and $J_{\beta_{\max}}(x)$ are reached at one and the same point, namely $x_{\max} = x_{\beta_{\max}}$. The solution to problem (31) continuously depends on β at any finite section $[\beta_1, \beta_2]$.

It follows from the lemma that it is possible to reduce the solution of extremum problem (30) to the solution of problem (31) for $\beta = \beta_{\max}$. The value of the numerical parameter $\beta_{\max}$ required for it can be found as the only solution to the equation $j(\beta) = 0$. it is clear that such a reduction can be efficient only when problems (31) are simpler to solve as compared to problems (30), e.g., when the numerator and the denominator of the functional J are linearly-quadratic functionals. In this case, the functional J_β is also a linearly-quadratic one. Thus, the problem of searching for a global extremum of the nonlinear functional J in the liner space of a large dimensionality can be reduced to a more elementary problem of searching for a global extremum of a quadratic functional and a further solution of this equation with respect to one unknown quantity that does not also require a hard computational burden.

REFERENCES

1. V. V. Goncharov, V. Yu. Zaĭtsev, V. M. Kurtepov, A. G. Nechaev, and A. I. Khil'ko, *Acoustic Tomography of Ocean* (IPF RAN, Novgorod, 1998) [in Russian].
2. A. G. Luchinin and A. I. Khil'ko, Akust. Zh. **51**, 124 (2005) [Acoust. Phys. **51**, 182 (2005)].
3. V. G. Burdukovskaya, A. G. Luchinin, A. I. Khil'ko, and I. P. Smirnov, Akust. Zh. **53**, 437 (2007) [Acoust. Phys. **53**, 381 (2007)].
4. V. I. Talanov, Preprint IPF AN SSSR (Gorky, 1984).
5. E. D. Gorodetskaya, A. I. Malekhanov, A. I. Talanov, and I. Sh. Fiks, in *Formation of Acoustic Fields in Oceanic Wave-Guides* (IPF RAN SSSR, Novgorod, 1991), pp. 9–31 [in Russian].
6. B. V. Kerzhakov, V. V. Kulinich, A. G. Koshkin, and A. I. Khil'ko, Izv. Vyssh. Uchebn. Zaved., Radiofiz. **49**, 770 (2006).
7. B. V. Kerzhakov, V. V. Kulinich, A. G. Koshkin, and A. I. Khil'ko, in *Proc. of the 10th School-Seminar of Acad. L.M. Brekhovskikh, with 14th Session of Russ. Acoust. Soc.* (GEOS, Moscow, 2004), pp. 206–210.
8. B. V. Kerzhakov, V. V. Kulinich, A. G. Koshkin, and A. I. Khil'ko, Izv. Vyssh. Uchebn. Zaved., Radiofiz. **49**, 925 (2006).
9. I. P. Smirnov, A. I. Khil'ko, and T. V. Romanova, Izv. Vyssh. Uchebn. Zaved., Radiofiz. **51**, 50 (2008).
10. L. M. Brekhovskikh and Yu. P. Lysanov, *Fundamentals of Ocean Acoustics* (Gidrometeoizdat, Leningrad, 1982; Springer-Verlag, New York, 1991).
11. G. P. Liu, J. B. Yang, and J. F. Whildborne, *Multiobjective Optimization and Control* (Res. Studies Press, Hertfordshire, England, 2003).
12. F. P. Vasil'ev, *Numerical Methods of Solution of Extremal Problems* (Nauka, Moscow, 1981) [in Russian].
13. P. Lancaster, *The Theory of Matrices* (Academic, New York, 1985; Nauka, Moscow, 1978).
14. A. N. Tikhonov and V. I. Dmitriev, in *Computational Methods and Programming* (Mosk. Gos. Univ., Moscow, 1969), pp. 209–214 [in Russian].
15. I. P. Smirnov, I. R. Smirnova, and A. I. Khil'ko, Preprint No. 786 (IPF RAN, Nizh. Novgorod, 2010).